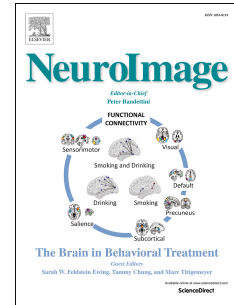


# Accepted Manuscript

Applying dimension reduction to EEG data by principal component analysis reduces the quality of its subsequent independent component decomposition

Fiorenzo Artoni, Arnaud Delorme, Scott Makeig



PII: S1053-8119(18)30214-3

DOI: [10.1016/j.neuroimage.2018.03.016](https://doi.org/10.1016/j.neuroimage.2018.03.016)

Reference: YNIMG 14785

To appear in: *NeuroImage*

Received Date: 19 September 2017

Revised Date: 8 February 2018

Accepted Date: 7 March 2018

Please cite this article as: Artoni, F., Delorme, A., Makeig, S., Applying dimension reduction to EEG data by principal component analysis reduces the quality of its subsequent independent component decomposition, *NeuroImage* (2018), doi: 10.1016/j.neuroimage.2018.03.016.

This is a PDF file of an unedited manuscript that has been accepted for publication. As a service to our customers we are providing this early version of the manuscript. The manuscript will undergo copyediting, typesetting, and review of the resulting proof before it is published in its final form. Please note that during the production process errors may be discovered which could affect the content, and all legal disclaimers that apply to the journal pertain.

1 **Applying dimension reduction to EEG data by Principal Component Analysis reduces the**  
2 **quality of its subsequent Independent Component decomposition**

3 Fiorenzo Artoni<sup>1,2,\*</sup>, Arnaud Delorme<sup>3,4,#</sup>, Scott Makeig<sup>3,#</sup>  
4  
5  
6

7 **Affiliations**

8 <sup>1</sup>The Biorobotics Institute, Scuola Superiore Sant'Anna, Pisa, Italy

9 <sup>2</sup>Translational Neural Engineering Laboratory, Center for Neuroprosthetics and Institute of  
10 Bioengineering, EPFL – Campus Biotech, Geneva, Switzerland

11 <sup>3</sup>Swartz Center for Computational Neuroscience, Institute for Neural Computation, University of California  
12 San Diego, La Jolla CA 92093-0559

13 <sup>4</sup>Univ. Grenoble Alpes, CNRS, LNPC UMR 5105, Grenoble, France.

14 \* Correspondence to: [fiorenzo.artoni@epfl.ch](mailto:fiorenzo.artoni@epfl.ch)

15 # Equal Contributors  
16

17 **Summary Sentences**

- 18 • It is currently a common practice to apply dimension reduction to EEG data using PCA before  
19 performing ICA decomposition.
- 20 • We tested the numbers and quality of meaningful Independent Components (ICs) separated from  
21 72-channel data after different levels of rank reduction to a principal subspace.
- 22 • PCA rank reduction (even if removing only 1% of data variance) adversely affected the dipolarity  
23 and stability of ICs accounting for potentials arising from brain and known non-brain processes.
- 24 • PCA rank reduction also increased uncertainty in the equivalent dipole positions and spectra of  
25 the IC brain effective sources across subjects.
- 26 • For EEG data at least, PCA rank reduction should therefore be avoided or at least carefully tested  
27 on each dataset before applying dimension reduction as a preprocessing step.  
28

**Abstract**

Independent Component Analysis (ICA) has proven to be an effective data driven method for analyzing EEG data, separating signals from temporally and functionally independent brain and non-brain source processes and thereby increasing their definition. Dimension reduction by Principal Component Analysis (PCA) has often been recommended before ICA decomposition of EEG data, both to minimize the amount of required data and computation time. Here we compared ICA decompositions of fourteen 72-channel single subject EEG data sets obtained (i) after applying preliminary dimension reduction by PCA, (ii) after applying no such dimension reduction, or else (iii) applying PCA only. Reducing the data rank by PCA (even to remove only 1% of data variance) adversely affected both the numbers of dipolar independent components (ICs) and their stability under repeated decomposition. For example, decomposing a principal subspace retaining 95% of original data variance reduced the mean number of recovered 'dipolar' ICs from 30 to 10 per data set and reduced median IC stability from 90% to 76%. PCA rank reduction also decreased the numbers of near-equivalent ICs across subjects. For instance, decomposing a principal subspace retaining 95% of data variance reduced the number of subjects represented in an IC cluster accounting for frontal midline theta activity from 11 to 5. PCA rank reduction also increased uncertainty in the equivalent dipole positions and spectra of the IC brain effective sources. These results suggest that when applying ICA decomposition to EEG data, PCA rank reduction should best be avoided.

**Keywords:**

Principal component analysis; PCA; Independent component analysis; ICA; electroencephalogram; EEG; Source Localization; Dipolarity; Reliability

## 1 I. Introduction

2 Over the last decade, Independent Component Analysis (ICA) has been steadily gaining popularity  
3 among blind source separation (BSS) techniques used to disentangle information linearly mixed into  
4 multiple recorded data channels so as to prepare multivariate data sets for more general data mining, in  
5 particular for electroencephalographic (EEG) data (Makeig et al., 1996; Makeig et al., 2002). In fact, Local  
6 Field activities at frequencies of interest (0.1 Hz to 300 Hz or beyond) arising from near-synchronous  
7 activity within a single cortical patch are projected by volume conduction and linearly mixed at scalp EEG  
8 channels (Nunez, 1981). A collection of concurrent scalp channel signals may be linearly transformed by  
9 ICA decomposition into a new spatial basis of maximally temporally independent component (IC)  
10 processes that can be used to assess individual EEG effective source dynamics without prior need for an  
11 explicit electrical forward problem head model (Makeig et al., 2004; Onton et al., 2006). Each IC is  
12 represented by its pattern of relative projections to the scalp channels (its 'scalp map') and by the time-  
13 varying signed strength of its equivalent source signal (Delorme et al., 2012). If electrode locations in the  
14 IC scalp maps are known, ICs representing cortical brain processes can typically be localized using either a  
15 single equivalent dipole model or a distributed source patch estimate (Acar et al., 2016).

16 As with most BSS algorithms, obtaining highly reliable extracted components is essential for their  
17 correct interpretation and use in further analysis. This is made difficult, however, by noise in the data  
18 (from small, irresolvable signal sources, the scalp/sensor interface, or the data acquisition system), by  
19 inadequate data sampling (e.g., when not enough data points are available to identify many independent  
20 source processes), by algorithmic shortcomings (e.g., convergence issues, response to local minima, etc.)  
21 and by inadequate data pre-processing (Artoni et al., 2014; Delorme et al., 2007; Jung et al., 2000). Several  
22 classes of stereotyped artifacts (e.g., scalp and neck muscle electromyographic (EMG) activities,  
23 electrocardiographic (ECG) signal contamination, single-channel noise produced by occasional disruption  
24 in the connections between the electrodes and the scalp, and electro-oculographic (EOG) activity  
25 associated with eye blinks, lateral eye movements, and ocular motor tremor) have been found to be well  
26 separated from brain activities in EEG data by means of ICA decomposition, provided enough adequately  
27 recorded and preprocessed data are available (Jung et al., 2000; Onton and Makeig, 2009).

28 For such data sets, a second subset of independent components (ICs) have scalp maps that highly  
29 resemble the projection of a single equivalent dipole located in the brain (or sometimes the summed  
30 projections of two equivalent dipoles, typically located near symmetrically with respect to the  
31 interhemispheric fissure). (Delorme et al., 2012) showed that the more mutual information between  
32 channel data time courses was reduced by the linear BSS transform the larger number of such 'dipolar'

1 component processes are present in the resulting ICs. Single equivalent dipole models have scalp maps  
2 mathematically *equivalent* to scalp projections of locally coherent (or near-coherent) cortical field activity  
3 within single cortical patches whose local spatial coherence also makes them relatively strong effective  
4 sources of scalp-recorded EEG signal (Acar et al., 2016; Scherg and Von Cramon, 1986).

5 Principal Component Analysis (PCA) has been widely used in various research fields (e.g.,  
6 electromyography, EMG) to reduce the dimensionality of the original sensor space and simplify  
7 subsequent analyses. By means of an orthogonal rotation, PCA linearly transforms a set of input data  
8 channels into an equal number of linearly-uncorrelated variables (Principal Components, PCs) that each  
9 successively account for the largest possible portion of remaining data variance (Kambhatla and Leen,  
10 1997). PCA has been used directly as a BSS method or as a preprocessing step. PCs have been proposed  
11 for use in extracting event-related potentials (ERPs) (Bromm and Scharein, 1982), in subsequent  
12 frequency domain analyses (Ghandeharion and Erfanian, 2010), or for the identification and removal of  
13 artifacts (Casarotto et al., 2004; Ghandeharion and Erfanian, 2010; Lagerlund et al., 1997). In other  
14 biomedical fields, PCA has been used, e.g., to increase signal-to-noise ratio (SNR) in evoked neuromagnetic  
15 signals (Kobayashi and Kuriki, 1999), and to identify muscle synergies in rectified EMG data, either in  
16 combination with Factor Analysis (FA) or to determine the optimal number of muscle synergies to extract,  
17 under the assumption that this information is captured by only a few PCs with high variance (Artoni et al.,  
18 2013; Ivanenko et al., 2004; Staudenmann et al., 2006). PCA has also been used to discriminate normal  
19 and abnormal gait based on vertical ground reaction force time series (Muniz and Nadal, 2009) and to set  
20 apart young and adult stair climbing gait patterns (Reid et al., 2010) or age-related kinematic gait  
21 parameters (Chester and Wrigley, 2008).

22 In these and other applications, PCA is used to reduce the dimension of the data. In such  
23 applications, the minimum set of largest PCs (i.e., the principal subspace) that accounts for at least some  
24 pre-defined variance threshold (usually in the range of 80% to 95% of original data variance) are  
25 considered for further analyses. In case of highly correlated data (e.g., 64-128 channel scalp EEG data), as  
26 few as 10-15 PCs may account for 95% of data variance. This PC subspace may then be given to an ICA (or  
27 similar) algorithm for further transformation with a goal of separating activities arising from different  
28 causes and cortical source areas. ICA decomposition minimizes the mutual information between the  
29 output component time courses, a stronger criterion than simply eliminating pairwise correlations.  
30 Reducing the input space can have the advantage of greatly reducing the computational load in  
31 subsequent processing, e.g., the time required for ICA decomposition to converge and the effort required  
to select which ICs to retain for further analysis (Artoni et al., 2014).

1 Perhaps for these reasons, most commercial software for EEG analysis advises users to reduce the  
2 data dimension using PCA so as to simplify the ICA component selection process and decrease processing  
3 time. The possibility of performing PCA during data preprocessing is left as a (non-default) user option in  
4 several ICA implementations, e.g. implementations of Infomax ICA (Bell and Sejnowski, 1995; Makeig et al.,  
5 1996) and FastICA (Hyvärinen and Oja, 2000), supported by open source EEG analysis environments  
6 (Delorme and Makeig, 2004; Oostenveld et al., 2011; Tadel et al., 2011).

7 For dimensionally redundant datasets, PCA dimension reduction may have a useful place. For  
8 example, re-referencing the data to the mean of two scalp channels (e.g., linked earlobes) will reduce the  
9 rank of a dataset by one. PCA can be used here to efficiently remove the introduced redundancy, making  
10 the data eligible for standard ‘complete’ (full-rank) ICA decomposition. Else, PCA might be used with very-  
11 short recordings to attenuate ICA convergence issues arising from data insufficiency. However, in these  
12 cases a viable and possibly preferable alternative is to reduce the number of data channels decomposed.

13 In a recent comparison of BSS methods applied to EEG data, PCA itself proved to be the least  
14 successful of 22 linear ICA/BSS algorithms at extracting physiologically plausible components, and by a  
15 considerable margin (Delorme et al., 2012). PCA also performed more poorly at extracting non-brain  
16 (artifact) sources from EEG data than infomax ICA (Jung et al., 1998). This is predictable from the  
17 objective of PCA, which can be said to be *to ‘lump’* as much scalp data variance as possible (from however  
18 many underlying sources) into each successive principal component (PC). ICA, on the other hand, tries to  
19 *‘split’* data variance into component pieces each associated with a single independent component (IC)  
20 process. However, the effects of (non-redundant) data dimension reduction by PCA on the quality and  
21 reliability of *subsequent* ICA decomposition of the rank-reduced data have not been reported.

22 If the channel data at hand in fact does represent summed mixtures of a small number of large,  
23 temporally independent source activities with near-orthogonal scalp maps, plus a large number of very  
24 small (‘noise’) sources of no particular interest, then performing data rank reduction to the dimension of  
25 the large sources using PCA might in some cases improve the signal-to-noise ratio of the large sources and  
26 subsequent recovery of the large sources of interest by ICA decomposition. However, when these  
27 conditions are not met (e.g., as is typical), when the data are produced by more sources than channels  
28 with a continuous range of amplitudes and non-orthogonal scalp projection patterns (scalp maps), then  
29 previous research suggests that PCA dimension reduction may adversely affect the quality of the ICA  
30 decomposition and, as well, the quality of the ICA-modeled results at subject group level.

31 Here we report testing this hypothesis by comparing the characteristics of ICA decompositions  
32 obtained after applying preliminary rank reduction using PCA (with retained data variances (RVs) of 85%,

1 95% and 99%) to those obtained by applying ICA or PCA only to the data. We tested the quality of the  
2 results in each case by using, as benchmark, the ‘dipolarity’ of the resulting ICs (a measure of their  
3 physiological plausibility) (Delorme et al., 2012), the stability of the ICs across bootstrap replications  
4 (Artoni et al., 2014), and group-level robustness of the resulting solutions (source localization, grand  
5 average topographies, and frequency spectra).

## 6 **II. Materials and Methods**

7 The analyses were performed on publicly available EEG data from fourteen subjects (see  
8 <http://sccn.ucsd.edu/wiki/BSSComparison>) acquired during a visual working-memory experiment  
9 approved by an Institutional Review board of the University of California San Diego. Further details may  
10 be found in (Delorme and Makeig, 2004; Onton et al., 2005). These data were also used by (Delorme et al.,  
11 2012) in their study, though as in (Artoni et al., 2014) we here included a data set, originally excluded in  
12 (Delorme et al., 2012) because of low data quality. All data and ICA decompositions are made available in  
13 (Artoni et al., 2018).

14 **The Experiment.** In brief, within each experimental trial the subject stared at a central fixation symbol  
15 for 5s (trial start), then a sequence of 3-7 letters were presented for 1.2s each with 200-ms gaps. The  
16 letters were colored according to whether they were to be memorized (black) or not (green). After a 2-4 s  
17 maintenance period, a probe letter was presented. The subject pressed one of two finger buttons with the  
18 dominant hand according to whether (s)he remembered the letter as having been in the memorized letter  
19 subset or not. Visual feedback was then provided as to the correctness of the response (a confirmatory  
20 beep or cautionary buzz). This also signaled trial end. The 14 subjects (7 males, 7 females, aged 20 – 40  
21 years) each performed 100-150 task trials.

22 The recorded data used here consisted of 100-150 concatenated 20-24s epochs per subject time  
23 locked to letter presentation events, recorded at 250 Hz per channel from 71 scalp channels (69 scalp and  
24 2 periocular electrodes, all referred to the right mastoid) and analog pass band of 0.01 to 100 Hz (SA  
25 Instrumentation, San Diego).

26 Subsequent data preprocessing, performed using MATLAB scripts using EEGLAB (version 14.x)  
27 functions (Delorme and Makeig, 2004), comprised (i) high-pass 0.5Hz FIR filtering, (ii) epoch selection ([-  
28 700 700] ms time locked to each letter presentation), (iii) whole-epoch mean channel (“baseline”) value  
29 removal, as this has been reported to give dramatically better ICA decomposition reliability and  
30 robustness to spatially non-stereotyped high-amplitude, high-frequency noise (i.e., without a spatially  
31 fixed distribution or source, such as produced by unconstrained cap movement) (Groppe et al., 2009).



1 **EEG data variance retained in a principal subspace.** Principal component Analysis (PCA) converts  
 2 observations of correlated variables into a set of linearly uncorrelated orthogonal variables (Principal  
 3 Components, PCs), ordered in such a way that each PC has the largest possible variance under the  
 4 constraint of being orthogonal to all preceding components. The first PC is not directionally constrained.  
 5 Both the time course and the scalp map of smaller PCs are orthogonal to the time courses and maps of all  
 6 other PCs. Because of this, the scalp maps of later PCs typically resemble checkerboard patterns. PCA can  
 7 serve both as an exploratory analysis tool and to provide a simplified visualization and interpretation of a  
 8 multivariate dataset. It has been proposed for use to decompose EEG and ERP data, most often followed  
 9 by further (orthogonal or non-orthogonal) adjustment (Dien et al., 2007).

10 Given a  $[n, t]$  mean-centered dataset  $X$  where  $n$  is the number of channels and  $t$  the number of  
 11 time points PCA is computed as the eigenvalue decomposition of the covariance matrix  $C_x = XX^T$ . The  
 12 portion of data variance accounted for the first  $p$  components, as a percent ratio with respect to the whole  
 13 dataset variance, is

$$RV_{1:p} = \frac{\sum_{i=1}^p \lambda_i}{\sum_{i=1}^n \lambda_i} 100\%$$

15 where  $\lambda_i$  is the eigenvalue associated with the  $i^{th}$  PC. Retaining a principal subspace of the data (i.e., some  
 16 number of largest PCs) that makes the retained data, when back-projected into its original channel basis,  
 17 exceed some specified percentage of the original data variance has been used extensively in different  
 18 fields to determine the number of PCs (and the concomitant amount of data variance) to retain for further  
 19 analysis. For instance, dimensionality reduction by PCA has been widely adopted for the extraction of  
 20 muscle synergies (modeled as PCs) from electromyography (EMG) using a threshold on cumulative  
 21 retained variance (RV), typically ranging from 75% to 95% of the original (Davis and Vaughan, 1993;  
 22 Shiavi and Griffin, 1981). The assumption is that small random fluctuations (i.e., noise) can be separated  
 23 from (relatively large) processes of interest (i.e., task-related information), and removed from the data by  
 24 discarding small PCs while retaining data variance to the given threshold value. PCA-based variance  
 25 reduction has also been used as a preprocessing step before applying other blind source separation  
 26 algorithms, e.g., Factor Analysis, Independent component Analysis (ICA), etc.

28 The EEG data were here PCA transformed including or not including the two bipolar electro-  
 29 oculographic (EOG) channels to determine whether this difference would affect the number of PCs needed



1 to reach a given RV threshold. For each subject, we created two datasets, one including and another not  
 2 including the two available (vertical and horizontal) electro-oculographic channels, and determined the  
 3 minimum number of PCs that jointly accounted for least 85%, 95%, 99% of data variance. The first two  
 4 thresholds are most often used in the literature; the latter we included to test whether even a quite small  
 5 decrease in RV can produce a difference in the number of *interpretable* EEG independent components  
 6 extracted from the data.

7 To test for differences among conditions, we first performed a one-sample Kolmogorov Smirnov  
 8 test (significance  $\alpha = 0.05$ ) which did not reject the (H0) hypothesis of Gaussianity. We then performed a  
 9 two-way ANOVA to test for effects of differences in RV threshold (1<sup>st</sup> level; 85%, 95%, 99%) and type of  
 10 preprocessing (2<sup>nd</sup> level; With versus Without EOG), followed by a post-hoc comparison (Tuckey's honest  
 11 significance difference criterion).

12 ***How does PCA affect the capability of ICA to extract interpretable brain and non-brain***  
 13 ***components?*** Blind source separation (BSS) methods such as PCA and Independent Component Analysis  
 14 (ICA), extract an  $[m \ n]$  "unmixing matrix"  $W$  where  $n$  is the number of channels and  $m$  the number of  
 15 independent components (ICs) retained so that

$$S = WX$$

17  
 18 where  $X$  is the original  $[n, t]$  dataset and  $S$  has dimensions  $[m, t]$ . The  $i^{th}$  row of  $S$  represents the time  
 19 course of the  $i^{th}$  IC (the IC's 'activation'). The "mixing matrix"  $A$  (the pseudoinverse of  $W$ ,  $A = W^+$ )  
 20 represents, column-wise, the weights with which the independent component (ICA) projects to the  
 21 original channels (the IC 'scalp maps'). For sake of simplicity, the terms "IC" will be used below for  
 22 components of PCA->ICA or ICA-Only origin, PCs for components of PCA-Only origin. Note that the  
 23 notation for PCA transformation differs from the ICA one, as in PCA-related papers the data  $X$  has  
 24 dimensions  $[t, n]$ ,  $S_{PCA} [t, m]$  and  $W_{PCA} [n, m]$  and therefore  $S_{PCA} = XW_{PCA}$ . In this notation, the data  
 25 channels are represented row-wise to adhere to ICA-related notation and to enhance the readability of the  
 26 manuscript.

27 If the electrode locations are available, the columns of  $A$  can be represented in interpolated  
 28 topographical plots of the scalp surface ("scalp maps") that are color-coded according to the relative  
 29 weights and polarities of the component projections to each of the scalp electrodes. While both

1 decompositions have the same linear decomposition form, PCA extracts components (PCs) with  
 2 *uncorrelated* time courses and scalp maps, while ICA extracts *maximally temporally-independent*  
 3 components (ICs) with unconstrained scalp maps. As linear decompositions, PCA and ICA can be used  
 4 separately, or PCA can be used as a preprocessing step to ICA to reduce the dimension of the input space  
 5 and speed ICA convergence.

$$S_{PCA} = W_{PCA}X$$

$$S_{ICA} = W_{ICA}X$$

$$S_{ICAPCA} = W_{ICA}S_{PCA} = W_{ICA}W_{PCA}X = W_{ICAPCA}X$$

7  
 8 Since the scalp maps of most effective brain source ICs strongly resemble the projection of a single  
 9 equivalent current dipole (Delorme et al., 2012), each component  $IC_n$  may be associated with a  
 10 “dipolarity” value, defined as the percent of its scalp map variance successfully explained by a best-fitting  
 11 single equivalent dipole model, here computed using a best-fitting spherical four/shell head model (shell  
 12 conductances: 0.33, 0.0042, 1, 0.33;  $\mu\text{S}$ , radii 71, 72, 79, 85) using the DIPFIT functions (version 1.02)  
 13 within the EEGLAB environment (Delorme and Makeig, 2004; Oostenveld and Oostendorp, 2002):

$$dip(IC_n) = 100(1 - resvar(IC_n))\%$$

14  
 15  
 16  $resvar(IC_n)$  being the fraction of residual variance explained by the equivalent dipole model,

$$resvar(IC_n) = \frac{var(ScalpMap(IC_n)) - var(DipoleMap(n))}{var(ScalpMap(IC_n))}$$

17  
 18  
 19 For ‘quasi-dipolar’ components with  $dip(IC_n) > 85\%$  and especially for ‘near-dipolar’ components  
 20 with  $dip(IC_n) > \sim 95\%$ , the position and orientation of their equivalent dipole is likely to mark the  
 21 estimated location of the component source (with an accuracy depending on the quality of the  
 22 decomposition and the accuracy of the forward-problem head model used to fit the dipole model). As  
 23 shown in Figure 3 of (Artoni et al., 2014), ICs with  $dip(IC_n) > 85\%$  have the lower likelihood of also

1 having a low quality index (meaning they have stability to resampling). In other words, highly dipolar ICs  
 2 are more likely to be stable than low dipolar ICs. As in (Delorme et al., 2012) and (Artoni et al., 2014),  
 3 here we define “decomposition dipolarity” as the number of ICs with a dipolarity value higher than a  
 4 given threshold (e.g., 85%, 95%).

5 To test how preliminary principal PCA subspace selection affects the capability of ICA to extract  
 6 meaningful artifact and brain components from EEG data, we applied ICA decomposition to each subject’s  
 7 dataset (i) after applying PCA and retaining 85%, 95%, or 99% of the data variance (PCA<sub>85</sub>ICA, PCA<sub>95</sub>ICA,  
 8 PCA<sub>99</sub>ICA); (ii) by performing ICA decomposition without preliminary PCA (ICA-Only); or (iii) by applying  
 9 PCA directly with no subsequent ICA (PCA-Only). In each case, we sorted quasi-dipolar ICs (defined here  
 10 as  $dip(IC_n) > 85\%$ ) into non-brain (“artifact”) and “brain” subsets, depending on the location of the  
 11 model equivalent dipole. The artifact subspace was mainly comprised of recurring, spatial stereotyped  
 12 (i.e., originating from a spatially fixed source) neck muscle activities or ocular movements. Example  
 13 results for one subject are shown in Figure 2.

14  
 15 **How does PCA preprocessing affect IC dipolarity?** After rejecting the null hypothesis of data  
 16 Gaussianity using a Kolmogorov Smirnov test (significance  $\alpha = 0.05$ ), we statistically compared the  
 17 number of dipolar ( $dip(IC_n) > 85\%$ ) and quasi-dipolar ( $dip(IC_n) > 95\%$ ) ICs, produced on average  
 18 across subjects by PCA-Only, ICA-Only, PCA<sub>85</sub>ICA, PCA<sub>95</sub>ICA, PCA<sub>99</sub>ICA. We used a Kruskal-Wallis test  
 19 followed by a Tuckey’s honest significant difference criterion for post-hoc comparison (Figure 3, left  
 20 panel).

21 To avoid limiting the generalizability of the results to dipolarity value thresholds of 85% and 95%,  
 22 we also compared the number of ICs with dipolarities larger than a range of thresholds ranging from 80%  
 23 to 99% in 1% increments. In particular, we performed the following comparisons: (i) PCA-Only versus  
 24 PCA<sub>85</sub>ICA; (ii) PCA<sub>85</sub>ICA versus PCA<sub>95</sub>ICA; (iii) PCA<sub>95</sub>ICA versus PCA<sub>99</sub>ICA; (iv) PCA<sub>99</sub>ICA versus ICA-Only.  
 25 We used a Wilcoxon signed rank test and reported the p-value for each dipolarity threshold value. A  
 26 significant p-value at some threshold T implies there were significantly different numbers of ICs with  
 27 dipolarity above T between conditions (PCA-Only versus PCA<sub>85</sub>ICA; PCA<sub>85</sub>ICA versus PCA<sub>95</sub>ICA). This test  
 28 enabled us to determine the exact dipolarity threshold above which the comparisons became non-  
 29 significant, that is the ‘significant dipolarity-difference’ point for each comparison (Figure 3, right panel).

30 We then estimated the probability density function (pdf) for dipolarity values across subjects in  
 31 PCA-Only, PCA<sub>85</sub>ICA, PCA<sub>95</sub>ICA, PCA<sub>99</sub>ICA and ICA-Only conditions using kernel density estimation

1 (Bowman and Azzalini, 1997) with a Gaussian kernel, which minimizes the (L2) mean integrated squared  
2 error (Silverman, 1986). We then estimated the median and skewness of the distribution (Figure 4).

3  
4 **How does PCA dimension reduction affect component stability?** To test the relative stability of ICs  
5 obtained after preliminary PCA processing versus ICs obtained by computing ICA directly on the data  
6 (ICA-Only), we used RELICA with trial-by-trial bootstrapping (Artoni et al., 2014). RELICA consists of  
7 computing  $W$  several times from surrogate data sets, formed by randomly selected epochs from the  
8 original data set with replacement, always replicating the original data set size.

9 For each subject, within RELICA we first performed PCA and retained the PCs, in decreasing order  
10 of variance, that explained at least 85%, 95%, or 99% variance of the original dataset. Then we applied  
11 RELICA using Infomax ICA (Bell and Sejnowski, 1995) in a 'beamICA' implementation (Kothe and Makeig,  
12 2013) after performing 50-fold trial-by-trial bootstrapping (Artoni et al., 2012), drawing points for each  
13 trial surrogate at random from the relevant trial with substitution. Infomax directly minimizes mutual  
14 information between component time courses (or, equivalently, maximizes the likelihood of the  
15 independent component model). Note that ICA is unaffected by the time order of the data points. In the  
16 ICA-Only condition, RELICA was applied directly to the original dataset as in (Artoni et al., 2014). RELICA  
17 tests the repeatability of ICs appearing in decompositions on bootstrapped versions of the input data to  
18 assess the stability of individual ICs to bootstrapping. In RELICA, the sets of ICs returned from each  
19 bootstrap decomposition are then clustered according to mutual similarity,  $\sigma$ , defined as the matrix of  
20 absolute values of the correlation coefficients between IC time courses, that is  $\sigma_{ij} = WR_{ij}W^T$  where  $R$  is  
21 the covariance matrix of the original data  $X$ . The number of clusters was chosen to be equal to the number  
22 of PCs back-projected to the scalp channels to create input to the ICA algorithm (or the number of scalp  
23 channels in condition ICA-Only). Clusters were identified using an agglomerative hierarchical clustering  
24 method, with group average-linkage criterion as agglomeration strategy; see (Artoni et al., 2014) for  
25 further details.

26 We used Curvilinear Component Analysis (CCA), a multidimensional scaling method, to project  
27 multivariate points into a two-dimensional space to obtain similarity maps (Himberg et al., 2004). The  
28 dispersion of each cluster was measured by the Quality Index (QIc), defined as the difference between the  
29 average within-cluster similarities and average between-cluster similarities.

$$QIc = 100 * \left( \frac{1}{|C_m|^2} \sum_{i,j \in C_m} \sigma_{ij} - \frac{1}{|C_m||C_{-m}|} \sum_{i,j \in C_m} \sum_{i,j \in C_{-m}} \sigma_{ij} \right)$$

1

2 where  $C_m$  is the set of IC indices that belong to the  $m^{th}$  cluster, and  $C_{-m}$  the set of indices that do not  
 3 belong,  $\sigma_{ij}$  the similarity between ICs  $i$  and  $j$ , and  $|\cdot|$  indicates the cardinality. The more compact the  
 4 cluster, the higher the QIc. A perfectly stable, repeatable component has a QIc of 100% (Figure 5).

5 As with dipolarity values, we estimated the probability density function (pdf) for QIc values over  
 6 all subjects in the PCA-Only, PCA<sub>85</sub>ICA, PCA<sub>95</sub>ICA, PCA<sub>99</sub>ICA and ICA-Only conditions and reported both the  
 7 median and skewness for each. After rejecting the null hypothesis of data Gaussianity using a Kolmogorov  
 8 Smirnov test (significance  $\alpha = 0.05$ ), we performed a non-parametric one-way analysis of variance  
 9 (Kruskal-Wallis-Test) on the QIc followed by a Tuckey-Kramer post-hoc comparison to highlight  
 10 significant difference and reported the ranks.

11 **How does PCA dimension reduction affect group-level results?** We tested the effects of PCA  
 12 preprocessing on the IC clusters, in particular on their spectra and grand-average cluster scalp maps at  
 13 group level. We examined the left mu ( $l\mu$ ) and frontal midline theta (FM $\theta$ ) components in the PCA<sub>85</sub>ICA,  
 14 PCA<sub>95</sub>ICA, PCA<sub>99</sub>ICA and ICA-Only conditions, as these ICs were of particular relevance to the brain  
 15 dynamics supporting the task performed by the subjects in the study (Onton et al., 2005). In each  
 16 condition, ICs for each subject were clustered using IC distance vectors combining differences in  
 17 equivalent dipole location, scalp projection pattern (scalp map) and power spectral density (1 - 45 Hz) for  
 18 each IC (Delorme and Makeig, 2004). Given the high dimensionality of the time and frequency features,  
 19 the dimensionality of the resulting joint vector was reduced to 15 principal components by PCA, which  
 20 explained 95% of the feature variance (Artoni et al., 2017). Vectors were clustered using a k-means  
 21 algorithm implemented in EEGLAB, ( $k = 15$ ). An “outliers” cluster collected components further than three  
 22 standard deviations from any of the resulting cluster center (Outlier ICs). We checked ICA decompositions  
 23 and added any seeming appropriate ICs left unclustered by the automated clustering procedure.

24 For each cluster ( $l\mu$  and FM $\theta$ ) and each condition, we then computed (i) the median absolute  
 25 deviation (MAD) of the distribution of the equivalent dipole positions ( $\sigma_x, \sigma_y, \sigma_z$ ) and (ii) the MAD of the  
 26 PSD ( $\sigma$ ) in the intervals 4 - 8 Hz and 9 - 11 Hz respectively for FM $\theta$  and  $l\mu$ . Figures 7 and 8 also report (i)  
 27 the single subject scalp topographies pertaining to the cluster; (ii) grand-average scalp topography; (iii)

1 cluster source location within a boundary element model based on the MNI brain template (Montreal  
2 Neurological Institute); (iv) median  $\pm$  MAD of the FM $\theta$  and  $\mu$  cluster PSDs across subjects (0 – 40 Hz).

### 4 III. Results

5 Results showed that, for all subjects, just  $8 \pm 2.5$  (median  $\pm$  MAD) PCs were needed to retain 95%  
6 of the EEG variance, regardless of whether the EOG data channels were or were not included in the data.  
7 Figure 1, panels A,B show a non-linear pattern of explained variance (RV%) with a saturation elbow  
8 between 5-10 PCs (85-95% RV%). Above PCA<sub>95</sub>ICA, an increasingly large number of components needed  
9 to be added to increase the RV%.

11 FIGURE 1 ABOUT HERE

13 **Extraction of brain and non-brain (artifact) components.** Figure 2 shows, for a representative  
14 subject, the scalp topographies of quasi-dipolar components (dipolarity > 85%), those extracted directly  
15 with PCA (PCA-only), directly by ICA (Infomax) without PCA, or by ICA after retaining the minimum  
16 number of PCs that explained 85% (PCA<sub>85</sub>ICA), 95% (PCA<sub>95</sub>ICA) and 99% (PCA<sub>99</sub>ICA) of dataset  
17 variance respectively. The quasi-dipolar ICs were then separated into 'brain ICs' (i.e., having a brain origin)  
18 and 'artifact (non-brain) ICs' mainly accounting for scalp/neck muscle and ocular movement artifact. For  
19 this subject only 3 components (PCs) extracted by PCA-only reached the 85% dipolarity threshold.  
20 Separate vertical and lateral eye movement ICs were extracted in the PCA<sub>85</sub>ICA, PCA<sub>95</sub>ICA and PCA<sub>99</sub>ICA,  
21 and ICA-Only conditions, but not in the PCA-Only condition. Left and right neck muscle components, as  
22 well as the left mu components were not extracted in either the PCA<sub>85</sub>ICA or PCA-Only conditions, and  
23 the higher the level of explained variance (RV) the less widespread the scalp maps (e.g., for those  
24 accounting for lateral eye movements). The number of artifact ICs as well as the number of brain ICs  
25 increased with the amount of variance retained (respectively, 3 non-brain, artifact and 3 brain ICs in  
26 RV85, 5 artifact and 5 brain ICs in PCA<sub>95</sub>ICA, 7 artifact and 12 brain ICs in PCA<sub>99</sub>ICA, and 12 artifact and  
27 15 brain ICs in ICA-Only).

29 FIGURE 2 ABOUT HERE

1

2 **Independent component dipolarity.** Over the whole subject pool, the left top (A) and bottom (B)  
 3 panels of Figure 3 show the box plot of the across-subjects median numbers of extracted quasi-dipolar  
 4 ( $dip(IC) > 85\%$ , top left panel A) and near-dipolar ( $dip(IC) > 95\%$ , bottom left panel B) ICs. Statistical  
 5 comparisons showed that the ICA-Only processing pipeline produced a significantly higher number of  
 6 quasi-dipolar and near-dipolar components than the pipelines PCA-Only, PCA<sub>85</sub>ICA, PCA<sub>95</sub>ICA ( $p < 0.001$ ),  
 7 and even PCA<sub>99</sub>ICA ( $p < 0.01$  for  $DIP \geq 85\%$ ,  $p < 0.05$  for  $DIP \geq 95\%$ ). The number of quasi- and near-dipolar  
 8 ICs in PCA<sub>99</sub>ICA was also significantly higher than in PCA<sub>95</sub>ICA, PCA<sub>85</sub>ICA, and PCA-Only ( $p < 0.0001$  for  
 9  $DIP \geq 85\%$ ,  $p < 0.001$  for  $DIP \geq 95\%$ ). No significant differences were found between the numbers of near-  
 10 dipolar ICs in the PCA-Only, PCA<sub>85</sub>ICA and PCA<sub>95</sub>ICA conditions. The dotted red lines in Figure 3 (A and B)  
 11 highlight a positive trend in the number of quasi-dipolar components, including a change of slope in  
 12 conditions PCA<sub>95</sub>ICA and PCA<sub>99</sub>ICA, as successive PCs are increasingly smaller themselves.

13 The right panels of Figure 3C show the estimated probabilities of significant difference in the  
 14 number of dipolar ICs for several pairwise condition contrasts for threshold values ranging from  $DIP > 80\%$   
 15 to  $DIP > 99\%$  (x axis). In the contrast between PCA-Only and PCA<sub>85</sub>ICA conditions, the significant  
 16 condition difference threshold ( $p < 0.05$ ) is never reached (top right panel). For other comparisons in  
 17 which ICA is used, significant condition differences appear for all but the following dipolarity threshold  
 18 values:  $DIP \geq 95\%$  (PCA<sub>85</sub>ICA versus PCA<sub>95</sub>ICA, second right panel) and  $DIP \geq 97\%$  (PCA<sub>95</sub>ICA versus  
 19 PCA<sub>99</sub>ICA, third right panel; PCA<sub>99</sub>ICA versus ICA-Only, bottom right panel). Panel D shows for each subject  
 20 the number of dipolar ICs (at thresholds  $DIP > 85\%$ , left panel;  $DIP > 95\%$ , right panel) against the number  
 21 of total ICs retained after applying PCA with PCA<sub>85</sub>ICA (black dots), PCA<sub>95</sub>ICA (green dots), PCA<sub>99</sub>ICA (blue  
 22 dots) and ICA only (red dots) respectively. For each subject, relative dots are connected by a dashed blue  
 23 line. The red dotted line delimits the region where the number of dipolar ICs is equal to the number of ICs.  
 24 The number of dipolar ICs increases monotonically and nonlinearly with the #ICs available. The sheaf of  
 25 lines is adherent to the delimitation line for #ICs  $< 20$  and  $DIP > 85\%$  and for #ICs  $< 10$  for  $DIP > 95\%$ .

26

27

FIGURE 3 ABOUT HERE

28

29 Figure 4 shows the distribution of dipolarities across all subject datasets. The skewness of the  
 30 distributions is negative ( $sk = -2.1$  for PCA<sub>85</sub>ICA,  $-1.5$  for PCA<sub>95</sub>ICA,  $-0.8$  for PCA<sub>99</sub>ICA and ICA-Only) for all



1 conditions involving ICA decomposition (i.e., except in PCA-Only,  $sk = +2.1$ ). The median dipolarity values  
2 for PCA→ICA pipelines range from 80% (ICA-Only and RV99%) to over 90% (PCA<sub>85</sub>ICA), whereas for  
3 PCA-Only, the median component dipolarity is near 12% (profoundly non-dipolar).

4  
5 FIGURE 4 ABOUT HERE

6  
7 **Independent component stability.** Figure 5 shows, for a representative subject, the dispersion of left  
8 hand-area (strong mu rhythm), central posterior (strong alpha activity), and eye blink artifact clusters in  
9 the two-dimensional CCA space computed by RELICA for four ICA-involved conditions. Note that the  
10 corresponding cluster quality (QIc) values for the visualized ICA-Only ICs (95%, 99%, and 98%) are  
11 higher than for corresponding ICs from the PCA<sub>85</sub>ICA (NA, 83%, 88%), PCA<sub>95</sub>ICA (83%, 81%, 89%) and  
12 PCA<sub>99</sub>ICA (78%, 85%, 89%) pipelines.

13  
14 FIGURE 5 ABOUT HERE

15  
16 This was confirmed by assessing the QIc distributions across subjects (Figure 6). The QIc  
17 distribution for ICA-Only is centered towards higher QIc values than for the other conditions as measured  
18 by the skewness (-0.3, -0.8, -0.6, and -1.9 for PCA<sub>85</sub>ICA, PCA<sub>95</sub>ICA, PCA<sub>99</sub>ICA and ICA-Only respectively).  
19 Figure 6 (bottom panel) shows that the median QIc in the ICA-Only condition was significantly higher  
20 ( $p < 0.001$ ) than for other conditions, while no significant difference appeared between the three PCA→ICA  
21 conditions. In other words, applying PCA dimension reduction during preprocessing, even while retaining  
22 99% of dataset variance, decreased the stability of the returned ICs.

23  
24 FIGURE 6 ABOUT HERE

25  
26 **Group-level results.** To determine the effects of PCA preprocessing on group-level results we analyzed  
27 IC clusters exhibiting clear left-hemisphere (right-hand) area (9-11 Hz) mu rhythm ( $\mu$ ) and frontal  
28 midline (4-8 Hz) theta band ( $fM\theta$ ) activities, respectively. Figure 7 shows the results of IC effective source  
29 clustering at the group level plus grand-average power spectral density for cluster  $fM\theta$ . While 11 of 14

1 subjects exhibited a clear frontal midline theta component activation in the ICA-Only condition  
 2 decompositions, the number of fM $\theta$  cluster ICs decreased to just 6 in PCA<sub>99</sub>ICA, to 5 in PCA<sub>95</sub>ICA, and to 4  
 3 in PCA<sub>85</sub>ICA. This means that for 5 of the subjects (11-6=5), fM $\theta$  ICs could be found only when the last 1%  
 4 of explained variance was included in the ICA decomposition, and for two more subjects only when at  
 5 least the next 4% (altogether, 95%) of data variance was retained (Figure 7, 1<sup>st</sup> column). The new fM $\theta$  ICs  
 6 recovered by the PCA<sub>95</sub>ICA and PCA<sub>99</sub>ICA decompositions were not themselves small. For example, a  $\mu$   
 7 IC that appeared in the PCA<sub>99</sub>ICA decomposition, but not in the PCA<sub>95</sub>ICA for one subject accounted for  
 8 over 6% of data variance – more than the additional amount of data variance retained in PCA<sub>99</sub>ICA versus  
 9 PCA<sub>95</sub>ICA.

10 While the grand-average cluster scalp maps (except in PCA<sub>85</sub>ICA) appear similar to one another,  
 11 the PCA<sub>99</sub>ICA condition cluster only includes contributions from half the subject population (versus 11 of  
 12 14 for ICA-Only). The cluster IC equivalent dipole locations for the fM $\theta$  cluster also had a higher median  
 13 absolute deviation (MAD) in PCA<sub>99</sub>ICA ( $\sigma_x = 4.5, \sigma_y = 15.1, \sigma_z = 20.1$ ), PCA<sub>95</sub>ICA ( $\sigma_x = 7.3, \sigma_y =$   
 14  $27.9, \sigma_z = 20.0$ ) and PCA<sub>85</sub>ICA ( $\sigma_x = 5.2, \sigma_y = 25.7, \sigma_z = 25.0$ ) than in the ICA-Only condition  
 15 ( $\sigma_x = 2.6, \sigma_y = 10.5, \sigma_z = 8.3$ ), indicating higher scattering of equivalent dipole effective source locations  
 16 across subjects when PCA dimension reduction was used (Figure 7, 3<sup>rd</sup> column). As well, the  $\theta$  peak in the  
 17 cluster mean PSD (Figure 7, 4<sup>th</sup> column) is sharper, and the PSD MAD lower, in the ICA-Only condition  
 18 ( $\sigma = 0.7$ ) than in the PCA $\rightarrow$ ICA conditions: PCA<sub>99</sub>ICA,  $\sigma = 0.9$ ; PCA<sub>95</sub>ICA,  $\sigma = 1.2$ ; PCA<sub>85</sub>ICA,  $\sigma = 3.2$ .

19  
 20 FIGURE 7 ABOUT HERE  
 21

22 Similar conclusions can be drawn for the left hand (right hemisphere) area  $\mu$  ( $\mu$ ) cluster. Figure  
 23 8 shows that the  $\mu$  cluster represents effective source activities from 8, 7, 6 and no subjects in the ICA-  
 24 Only, PCA<sub>99</sub>ICA PCA<sub>95</sub>ICA and PCA<sub>85</sub>ICA conditions, respectively (no  $\mu$  cluster was found in the PCA<sub>85</sub>ICA  
 25 ICs). The  $\mu$  cluster equivalent dipole MAD is ( $\sigma_x = 5.7, \sigma_y = 11.0, \sigma_z = 7.6$ ) in ICA-Only, ( $\sigma_x = 7.4, \sigma_y =$   
 26  $8.8, \sigma_z = 7.9$ ) in PCA<sub>99</sub>ICA, and ( $\sigma_x = 11.7, \sigma_y = 11.0, \sigma_z = 14.4$ ) in PCA<sub>95</sub>ICA. Regarding the PSD, the beta  
 27 band peak in the PSD (18-24 Hz range) can only be seen clearly in results from ICA-Only. The MAD of the  
 28 PSD also increases as ICA is applied to smaller principal subspaces of the data:  $\sigma = 1.7$  for ICA-Only;  
 29  $\sigma = 2.5$  for PCA<sub>99</sub>ICA;  $\sigma = 2.6$  for PCA<sub>95</sub>ICA.  
 30

FIGURE 8 ABOUT HERE

#### IV. Discussion

**PCA-based rank reduction affects the capability of ICA to extract dipolar brain and non-brain (artifact) components.** Figure 1 shows a nonlinear relationship between cumulative retained variance and the number of PCs retained. Here a ten-dimension principal subspace (the first 10 PCs) comprised as much as 95% of the ~70-channel dataset variance. To increase the variance retained by another 4%, 15 more (smaller) PCs were required, and 15 more (smaller still) were needed to reach 99%. The first (largest) PCs were likely dominated by large ocular and other non-brain artifacts, as there were no significant differences in cumulative variance retained depending on whether EOG channels were included in or excluded.

The aim of principal component analysis is to extract both spatially and temporally orthogonal components, each in turn maximizing the amount of additional variance they contribute to the accumulating principal subspace. This process can be characterized as “lumping” together portions of the activities of many temporally independent, physiologically and functionally distinct, but spatially non-orthogonal effective IC sources. Fulfilling this objective means that, typically, low-order principal components are dominated by large, typically non-brain artifact sources such as eye blinks (Möcks and Verleger, 1986), while high-order principal component scalp maps resemble checkerboards of various densities.

Figure 4 shows the pooled dipolarity distribution of ICs and PCs across the subjects. For PCs, this distribution is centered on low values (near 10%, highly incompatible with a single source equivalent dipole) and has high positive skewness (2.1). ICA, by maximizing signal independence and removing the orthogonality constraint on the component scalp maps, also produces many ICs with high scalp map dipolarity, producing a dipolarity distribution with high median (about 90%) and negative skewness. This result is in accord with (Delorme et al., 2012) who discovered a positive linear correlation, for some 18 linear decomposition approaches, between the amount of mutual information reduction (between time courses) produced in linearly transforming the data from a scalp channel basis to a component basis, and the number of near-dipolar components extracted.

As a further confirmation of this, here only three dipolar PCs on average could be extracted from each subject by PCA-Only (Figures 2 and 3). The scalp map of the first PC resembles the scalp projection of lateral eye movement artifact; the second PC appears to combine scalp projections associated with vertical

1 eye movement artifact (e.g., IC1 in PCA<sub>85</sub>ICA), alpha band activity (IC1, PCA<sub>95</sub>ICA) and neck muscle artifact  
2 (neck muscle IC7, PCA<sub>99</sub>ICA).

3 Any full-rank, well-conditioned preliminary linear transformation of the data (e.g., PCA with 100%  
4 variance retained) does not affect ICA results. Also, variance alone is insufficient for separating  
5 physiologically meaningful components and noise (Kayser and Tenke, 2006). As it is, by reducing the rank  
6 of the data by PCA before applying ICA also reduced the number of brain and non-brain artifact dipolar ICs  
7 that were extracted. Figure 2 shows that ICs accounting for vertical and lateral eye movement artifacts  
8 (blue dashed box) were always extracted. However, for the lateral eye movement component, the higher  
9 the retained variance, the less affected the channels other than the frontal ones.

10 Figure 3 (panels A, B) shows the median numbers of quasi-dipolar (DIP  $\geq$  85%) and near-dipolar  
11 (DIP  $\geq$  95%) ICs, respectively, that were extracted depending on the amount of retained variance.  
12 Statistical analysis showed a significant increase ( $p < 0.01$  for DIP  $\geq$  85%,  $p < 0.05$  for DIP  $\geq$  95%) in the  
13 numbers of dipolar components produced by ICA-Only in comparison to PCA<sub>99</sub>ICA. The number of  
14 retained PCs affects the number of dipolar ICs that ICA can extract subsequently. Using a stricter near-  
15 dipolar threshold (DIP  $\geq$  95%), the increasing numbers of dipolar ICs returned on average by PCA<sub>95</sub>ICA,  
16 PCA<sub>99</sub>ICA, and ICA-Only for the 14 subjects were 4, 6, and 9 respectively. Using the looser quasi-dipolar  
17 threshold (DIP  $\geq$  85%), the larger numbers of ICs rated as dipolar (8, 23, 31) were less dramatically  
18 affected by dimension reduction (Figure 3). Condition-to-condition differences in numbers of returned  
19 'dipolar' components (Figure 3C) were statistically significant for all but the strictest dipolarity thresholds  
20 (reached by relatively few ICs in any condition).

21 The paucity of near-dipolar ICs likely in part arises from disparities between the common MNI  
22 template electrical head model used here to compute dipolarity values and more accurate individualized  
23 head models (e.g. built from subject MR head images). In Fig. 3C, PCA<sub>85</sub>ICA never produces significantly  
24 more dipolar ICs than PCA-Only; evidently, retaining only 85% of explained variance (e.g., within the first  
25 10 PCs) left too few degrees of freedom for the ICA algorithm to be able to extract a significantly higher  
26 number of dipolar ICs than PCA alone.

27 In other words, the extra degrees of freedom allowed by higher retained variances (ideally 100%,  
28 i.e., without applying PCA dimension reduction at all), allows ICA to re-distribute data variance to achieve  
29 stronger MI reduction, thereby separating more component processes compatible with spatially coherent  
30 activity across a single cortical patch. The significant differences, at all dipolarity threshold values lower  
31 than DIP > 97%, in the numbers of dipolar components in PCA<sub>99</sub>ICA versus ICA-Only, shows the importance

1 for ICA effectiveness of keeping the whole data intact rather than reducing it, even slightly, to a principal  
2 subspace.

3 The caution raised by these results concerning PCA dimension reduction prior to ICA  
4 decomposition of EEG data raises questions concerning other types of biological time series data to which  
5 ICA can be usefully applied, for example fMRI (McKeown et al., 1997), MEG (Iversen and Makeig, 2014;  
6 Vigário et al., 1998), ECoG (Whitmer et al., 2010). Experience suggests to us that the same may be true for  
7 data reduction by (low-pass) frequency band filtering, although here we find that removing (often large)  
8 low-frequency activity below  $\sim 1$  Hz before ICA decomposition may improve, rather than degrade, success  
9 in returning dipolar ICs. This might reflect the differing origins and possible spatial non-stationary of low-  
10 frequency EEG processes, an assumption that needs more detailed testing. Based on experience and  
11 consistent with the results reported in (Winkler et al., 2015) we would recommend applying ICA on  $\sim 1$ -  
12 Hz high-passed data and, if different preprocessing steps are required (e.g., different high-pass filtering  
13 cutoff frequencies, different artifact removal pipelines), consider re-applying the model weights to the  
14 unfiltered raw data (e.g., to remove blinks from low-frequency activity)(Artoni et al., 2017). However,  
15 note that in this case one may not assume that the low-frequency portions of the signals have necessarily  
16 been correctly decomposed into their functionally distinct source processes, since some other low-  
17 frequency only processes may contribute to the data. It is also important to note that avoiding PCA as a  
18 preprocessing step does not guarantee a high-quality ICA decomposition, as quality is also affected also by  
19 other factors including inadequate data sampling (e.g., number of channels and/or effective data points  
20 available), inadequate data pre-processing, algorithm deficiencies and noise (Artoni et al., 2014). One of  
21 the reasons behind the application of PCA rank reduction by many users before ICA decomposition is  
22 likely the easier interpretation of a lower number of components. However, fixing the PCA variance  
23 threshold introduces variability in the number components available for each dataset and vice versa fixing  
24 the rank results in explained variance variability across datasets. A number of methods, that of Winkler et  
25 al. for one (Winkler et al., 2011), are available to aid in IC selection or classification.

26 For EEG data, valuable information about component process independence is contained in the  
27 final 1% of data variance (projected from the smallest PCs), and reducing the rank of the data so as to  
28 retain even as much as 99% of its variance impairs the capability of ICA to extract meaningful dipolar  
29 brain and artifact components. A principal reason for this is that PCA rank reduction increases the EEG  
30 overcompleteness problem of there being more independent EEG effective sources than degrees of  
31 freedom available to separate them. The objective of PCA to include as much data variance as possible in  
each successive PC, combined with the influence this entails on PCs to have mutually orthogonal scalp

1 maps, means that PCs almost never align with a single effective source (unless one source is much larger  
2 than all others and so dominates the first PC). That is, typically some portions of the activities of many the  
3 independent effective sources are summed in every PC. Choosing a PC subset reduces the number of  
4 degrees of freedom available to ICA while typically *not* reducing the number of effective brain and non-  
5 brain sources contributing to the channel data. Because principal component scalp maps must also be  
6 mutually orthogonal, scalp maps of successively smaller PCs typically have higher and higher spatial  
7 frequencies (and ‘checkerboard’ patterns). While PCA rank reduction might not degrade highly  
8 stereotyped components such as eye blinks, not removing small (high spatial-frequency) PCs from the  
9 data allows ICA to return dipolar IC scalp maps whose spatial frequency profiles, dominated by low  
10 (broad) spatial frequencies typical of dipolar source projections, conform more precisely to the true scalp  
11 projection patterns of the independent cortical and non-brain effective source processes.

12 ***PCA-based rank reduction decreased IC reliability across subjects.*** Measures of IC dipolarity and  
13 stability to data resampling are both important to assessment of *within*-subject IC reliability. While IC  
14 dipolarity provides a measure of physiological plausibility (Delorme et al., 2012), IC stability measures  
15 robustness to small changes in the data selected for decomposition (Artoni et al., 2014). Assessing IC  
16 reliability (dipolarity and stability) at the single-subject level is important to avoid mistakenly entering  
17 unreliable or physiologically uninterpretable ICs into group-level analyses.

18 Figure 5 shows the two-dimensional CCA cluster distributions and exemplar IC scalp maps for  
19 three IC clusters accounting for left mu, central alpha, and eye blink artifact activities respectively. As  
20 shown there, for ICA-Only the cluster quality indices for the three example clusters are in the 95-99%  
21 range, while for the three PCA→ICA conditions the equivalent component cluster quality indices range  
22 from only 78% to 89%, meaning that the IC time courses within bootstrap repetitions of the ICA  
23 decomposition (represented by dots in the Fig. 5 CCA plane plots) are less distinctly more correlated  
24 within-cluster versus between-clusters. The IC clusters appear more crisply defined in the CCA plane for  
25 ICA-Only (though note its larger data rank and, therefore, larger number of ICs). Figure 6 shows that  
26 across subjects, brain source ICs had a higher quality index  $Q_{IC}$  in the ICA-Only condition, for which the  
27 distribution was strongly skewed toward high  $Q_{IC}$  (skewness, -1.9; median  $Q_{IC}$ , 90%, significantly higher  
28 [ $p < 0.001$ ] than for the three PCA→ICA conditions). The  $Q_{IC}$  indirectly indexes the variability of the ICA  
29 decomposition by measuring the dispersion of an IC cluster within the 2-D CCA measure space (Artoni et  
30 al., 2014). Sources of variability in the ICA decomposition are noise, algorithm convergence issues (e.g.,  
31 local minima), non-stationary artifacts etc. Applying PCA dimension reduction with a specific RV%



1 threshold, makes ICA operate on a somewhat different data sample in each bootstrap repetition, thus  
2 likely introducing a further source of variability and further decreasing the QIc.

3 ***PCA-based rank reduction degraded the group-level results.*** The quality of information provided  
4 by group-level results depends on the reliability (dipolarity and stability) of the individual ICs, as  
5 supported by the results shown in Figures 7 and 8. For the frontal midline theta cluster (Figure 7), the  
6 lower the PCA-retained variance, the fewer the subjects represented in the cluster (e.g., 11 of 14 for ICA-  
7 Only versus 4 of 14 for PCA<sub>85</sub>ICA). For the mu cluster, in PCA<sub>85</sub>ICA no ICs reached the DIP > 85%  
8 threshold. Lack of uniform group representation is a distinct complication for performing group statistical  
9 comparisons on ICA-derived results, as modern statistical methods taking into account missing data  
10 should then be used (Dempster et al., 1977; Hamer and Simpson, 2009; Sinharay et al., 2001).

11 Cluster mean scalp maps (Fig. 7, 2<sup>nd</sup> column,) are also affected by the lower IC representation. The  
12 blue color of the average scalp map (PCA<sub>85</sub>ICA) over the occipital area is symptom of spurious brain  
13 activity captured by the cluster, other than the frontal midline theta (Onton et al., 2005). This is confirmed  
14 by source localization (Figures 7 and 8, 3<sup>rd</sup> column): equivalent dipoles are more scattered with PCA<sub>85</sub>ICA  
15 (only frontal midline theta), PCA<sub>95</sub>ICA than with PCA<sub>99</sub>ICA and ICA-Only. The lower the variance retained,  
16 the higher the standard errors,  $\sigma_x, \sigma_y, \sigma_z$ . While this might be ascribed to the lack of representation of the  
17 cluster by a sufficient number of ICs for PCA<sub>85</sub>ICA, the higher size of the cluster with lower RV% seems to  
18 confirm that ICs are not as well localized as with, e.g., ICA-Only, which suggests a relation between the  
19 total number of dipolar and reliable ICs obtained over all subjects and the source localization variability  
20 for group-level clusters. Source localization variability depends on many factors, e.g., inter-subject  
21 variability arising from different cortical convolutions across subjects, unavailability of MRI scans and  
22 electrode co-registration, source localization algorithm deficiencies, etc. However, preliminary rank  
23 reduction by PCA can further increase source position variability and impair the possibility to draw  
24 conclusions at group level.

25 Rank reduction also impacts task-based measures such as power spectral densities (PSDs). The  
26 variability across subjects in the theta band across subjects (Figure 7, 4th column) is maximum for  
27 PCA<sub>85</sub>ICA and minimum for ICA-Only (which here also produced a visually more pronounced theta peak).  
28 The same is true for the mu IC (Figure 8, 4th column): the typical 18-20 Hz second peak is clearly visible in  
29 the ICA-Only results, while it is barely hinted for PCA<sub>99</sub>ICA and does not appear for PCA<sub>95</sub>ICA. This result  
30 shows that rank reduction can have unpredictable effects not only on source localization and reliability of  
31 ICs but also on dynamic source measures such as PSD.



**Conclusion.** These results demonstrate that reducing the data rank to a principal subspace using PCA, even to remove as little as 1% of the original data variance, can adversely affect both the dipolarity and stability of independent components (ICs) extracted thereafter from high-density (here, 72-channel) EEG data, as well as degrading the overall capability of ICA to separate functionally identifiable brain and non-brain (artifact) source activities at both the single subject and group levels. These conclusions might vary slightly depending on the amount of data available (its length and number of channels), preprocessing pipeline, type of subject task, etc. Further work will focus on testing the extensibility of these findings to low-density (e.g., 16-32 channel), ultra-high-density (128+ channel), brief (too few 10 minutes) and lengthy (e.g., several hour) recordings. However, it is possible to conclude that contrary to common practice in this and related research fields, PCA-based dimension reduction of EEG data should be avoided or at least carefully considered and tested on each dataset before applying it during preprocessing for ICA decomposition.

### Funding and Acknowledgments

Dr. Artoni's contributions were supported by the European Union's Horizon 2020 research and innovation programme under Marie Skłodowska Curie grant agreement No. 750947 (project BIREHAB). Drs. Makeig and Delorme's contributions were supported by a grant (R01 NS047293) from the U.S. National Institutes of Health (NIH) and by a gift to the Swartz Center, UCSD from The Swartz Foundation (Old Field NY). We acknowledge Dr. Makoto Miyakoshi for his support and helpful discussions.

### Figure captions

**Figure 1:** Mean explained variance (blue line) in relation to the number of largest principal components (PCs) retained, including (A) or not including (B) the bipolar vertical and horizontal electro-oculographic channels (EOG<sub>v</sub> and EOG<sub>h</sub>). Panel C shows the average number of PCs necessary to explain at least 85%, 95%, 99% of original dataset variance, including (green) or not including (blue) the EOG.

**Figure 2:** For a representative subject, scalp maps of quasi-dipolar components (dipolarity above 85%) extracted by applying ICA (ICA-Only) or PCA (PCA-Only) directly to the data, or by performing ICA after reducing the original data rank by PCA so as to retain at least 85% (PCA85ICA,  $4 \pm 0.5$  Median  $\pm$  MAD PCs), 95% (PCA95ICA,  $8 \pm 2.5$  PCs) and 99% (PCA99ICA,  $21 \pm 6$  PCs) of data variance respectively. Components are sorted into identifiable non-brain Artifact and Brain ICs, separated by the vertical red dashed line. A

1 dashed blue box highlights eye activity-related artifact ICs (vertical EOG and horizontal EOG ICs,  
2 respectively) in the PCA95ICA, PCA99ICA, and ICA-Only conditions.

3  
4 **Figure 3: Panels A and B:** box plots of median numbers of ICs (#ICs) with dipolarity values (A) above 85%  
5 (quasi-dipolar) and (B) 95% (near-dipolar). Significance of differences between conditions was  
6 determined using Kruskal-Wallis plus Tuckey post hoc tests. **Panel C:** Estimated probabilities of  
7 significant condition differences in the number of quasi-dipolar components ( $RV > 85\%$ ) for the following  
8 comparisons: (i) PCA-Only versus PCA85ICA; (ii) PCA85ICA versus PCA95ICA; (iii) PCA95ICA versus  
9 PCA99ICA; (iv) PCA99ICA versus ICA-Only. Each panel shows p-values for existence of significant  
10 differences between the number of quasi-dipolar components in the contrasted condition pair for each  
11 dipolarity threshold (x axis,  $RV > 80\%$  to  $RV > 99\%$ ). Dashed red lines show the dipolarity condition-  
12 difference significance threshold (red dashed line at  $p=0.05$ ). **Panel D:** Numbers of dipolar ICs (y axis)  
13 available after PCA dimensionality reduction for two dipolarity thresholds (dipolarity  $> 85\%$ ,  $>95\%$ ) in  
14 decomposition conditions PCA85ICA (black dots), PCA95ICA (green dots), PCA99ICA (blue dots), and ICA-  
15 only (red dots). A dashed blue line connects the dots for each subject. A red dashed line plots the #ICs (the  
16 upper bound to the #dipolar ICs).

17  
18 **Figure 4:** Histograms of component dipolarities (across all 14 data sets) following preliminary PCA  
19 subspace restriction (to  $RV > 85\%$ ,  $RV > 95\%$ , or  $RV > 99\%$ ), without preliminary PCA (ICA-Only), or directly  
20 applying PCA (PCA-Only). The median of each distribution is indicated by a red vertical line (sk =  
21 skewness). Note the different y-axis scales.

22  
23 **Figure 5:** IC clusters extracted by RELICA bootstrap decompositions for one subject, either following  
24 reduction of data rank to a principal subspace (PCA<sub>85</sub>ICA, PCA<sub>95</sub>ICA and PCA<sub>99</sub>ICA) or (lower right)  
25 without PCA-based rank reduction. Within each box, the ICs are clustered according to mutual similarity  
26 and cluster quality index (QIc) values are computed to measure their compactness. At far left and right,  
27 scalp maps of example components in clusters associated with left hand-area (8-12 Hz) mu rhythm  
28 activity, central posterior (8-12 Hz) alpha band activity, and eye blink artifact are shown and their QIc  
29 values are indicated. Note the stronger between-subject cluster definition and higher QIc values  
30 (reflecting more highly correlated time course) for the IC clusters without PCA processing (ICA-Only,  
31 lower right).

1 **Figure 6:** Distribution of IC QIc values across the subjects for different levels of principal subspace data  
 2 variance retained (PCA<sub>85</sub>ICA, PCA<sub>95</sub>ICA, PCA<sub>99</sub>ICA) and for ICA-Only (100%). The median of each  
 3 distribution is indicated by a red vertical line (med = median; sk = skewness). **Bottom panel:** Significance  
 4 of pairwise differences between conditions, determined using a Kruskal-Wallis test with Tuckey post hoc  
 5 correction for multiple comparisons correction (\*\*\*) =  $p < .001$ .

6  
 7  
 8 **Figure 7:** The frontal midline theta (fM $\theta$ ) cluster identified across subjects in each of the four  
 9 decomposition conditions (PCA<sub>85</sub>ICA, PCA<sub>95</sub>ICA, PCA<sub>99</sub>ICA and ICA-Only) conditions. The picture shows the  
 10 individual IC scalp maps (1<sup>st</sup> column), the cluster-mean maps (2<sup>nd</sup> column), IC equivalent dipole locations  
 11 (3<sup>rd</sup> column – each dot represents one IC for one subject). The median absolute deviations  
 12 (MAD;  $\sigma_x, \sigma_y, \sigma_z$  in mm) of the cluster IC equivalent dipole positions are given. The 4<sup>th</sup> column shows  
 13 cluster median power spectral densities (PSDs, with  $\pm$  MAD shaded).  $\sigma_\theta$ , the MAD of the PSD in the (4-8 Hz)  
 14 theta band is also indicated.

15  
 16 **Figure 8:** Left mu clusters across all subjects for the PCA<sub>85</sub>ICA, PCA<sub>95</sub>ICA, PCA<sub>99</sub>ICA and ICA-Only  
 17 decomposition pipelines. The picture shows the individual IC scalp maps (1<sup>st</sup> column), cluster mean scalp  
 18 map (2<sup>nd</sup> column), IC equivalent dipole locations (3<sup>rd</sup> column – each dot represents an IC of one subject),  
 19 and in the 4<sup>th</sup> column, the cluster median ( $\pm$  9-11 Hz MAD) PSD. This is another example of the effects of  
 20 PCA dimension reduction at the across-subjects cluster level (cf. Figure 7).

## 22 References

23  
 24 Acar, Z.A., Acar, C.E., Makeig, S., 2016. Simultaneous head tissue conductivity and EEG source location  
 25 estimation. *Neuroimage* 124, 168-180.

26 Artoni, F., Delorme, A., Makeig, S., 2018. A visual working memory dataset collection with bootstrap  
 27 Independent Component Analysis for comparison of electroencephalogram preprocessing pipelines. *Data In*  
 28 *Brief Submitted*.

29 Artoni, F., Fanciullacci, C., Bertolucci, F., Panarese, A., Makeig, S., Micera, S., Chisari, C., 2017. Unidirectional  
 30 brain to muscle connectivity reveals motor cortex control of leg muscles during stereotyped walking.  
 31 *Neuroimage* 159, 403-416.

32 Artoni, F., Gemignani, A., Sebastiani, L., Bedini, R., Landi, A., Menicucci, D., 2012. ErpICASSO: a tool for  
 33 reliability estimates of independent components in EEG event-related analysis. *Conf Proc IEEE Eng Med Biol*  
 34 *Soc* 2012, 368-371.

- 1 Artoni, F., Menicucci, D., Delorme, A., Makeig, S., Micera, S., 2014. RELICA: a method for estimating the  
2 reliability of independent components. *Neuroimage* 103, 391-400.
- 3 Artoni, F., Monaco, V., Micera, S., 2013. Selecting the best number of synergies in gait: preliminary results on  
4 young and elderly people. *IEEE Int Conf Rehabil Robot* 2013, 6650416.
- 5 Bell, A.J., Sejnowski, T.J., 1995. An information-maximization approach to blind separation and blind  
6 deconvolution. *Neural Comput* 7, 1129-1159.
- 7 Bowman, A.W., Azzalini, A., 1997. Applied smoothing techniques for data analysis: the kernel approach with S-  
8 Plus illustrations. OUP Oxford.
- 9 Bromm, B., Scharein, E., 1982. Principal component analysis of pain-related cerebral potentials to mechanical  
10 and electrical stimulation in man. *Electroencephalography and clinical neurophysiology* 53, 94-103.
- 11 Casarotto, S., Bianchi, A.M., Cerutti, S., Chiarenza, G.A., 2004. Principal component analysis for reduction of  
12 ocular artefacts in event-related potentials of normal and dyslexic children. *Clinical neurophysiology* 115, 609-  
13 619.
- 14 Chester, V.L., Wrigley, A.T., 2008. The identification of age-related differences in kinetic gait parameters using  
15 principal component analysis. *Clinical Biomechanics* 23, 212-220.
- 16 Davis, B.L., Vaughan, C.L., 1993. Phasic behavior of EMG signals during gait: use of multivariate statistics.  
17 *Journal of Electromyography and Kinesiology* 3, 51-60.
- 18 Delorme, A., Makeig, S., 2004. EEGLAB: an open source toolbox for analysis of single-trial EEG dynamics  
19 including independent component analysis. *J Neurosci Methods* 134, 9-21.
- 20 Delorme, A., Palmer, J., Onton, J., Oostenveld, R., Makeig, S., 2012. Independent EEG sources are dipolar.  
21 *PLoS One* 7, e30135.
- 22 Delorme, A., Sejnowski, T., Makeig, S., 2007. Enhanced detection of artifacts in EEG data using higher-order  
23 statistics and independent component analysis. *Neuroimage* 34, 1443-1449.
- 24 Dempster, A.P., Laird, N.M., Rubin, D.B., 1977. Maximum likelihood from incomplete data via the EM  
25 algorithm. *Journal of the royal statistical society. Series B (methodological)*, 1-38.
- 26 Dien, J., Khoe, W., Mangun, G.R., 2007. Evaluation of PCA and ICA of simulated ERPs: Promax vs. Infomax  
27 rotations. *Human brain mapping* 28, 742-763.
- 28 Ghandeharion, H., Erfanian, A., 2010. A fully automatic ocular artifact suppression from EEG data using higher  
29 order statistics: Improved performance by wavelet analysis. *Medical engineering & physics* 32, 720-729.
- 30 Groppe, D.M., Makeig, S., Kutas, M., 2009. Identifying reliable independent components via split-half  
31 comparisons. *Neuroimage* 45, 1199-1211.
- 32 Hamer, R.M., Simpson, P.M., 2009. Last observation carried forward versus mixed models in the analysis of  
33 psychiatric clinical trials. *Am Psychiatric Assoc.*
- 34 Himberg, J., Hyvärinen, A., Esposito, F., 2004. Validating the independent components of neuroimaging time  
35 series via clustering and visualization. *Neuroimage* 22, 1214-1222.

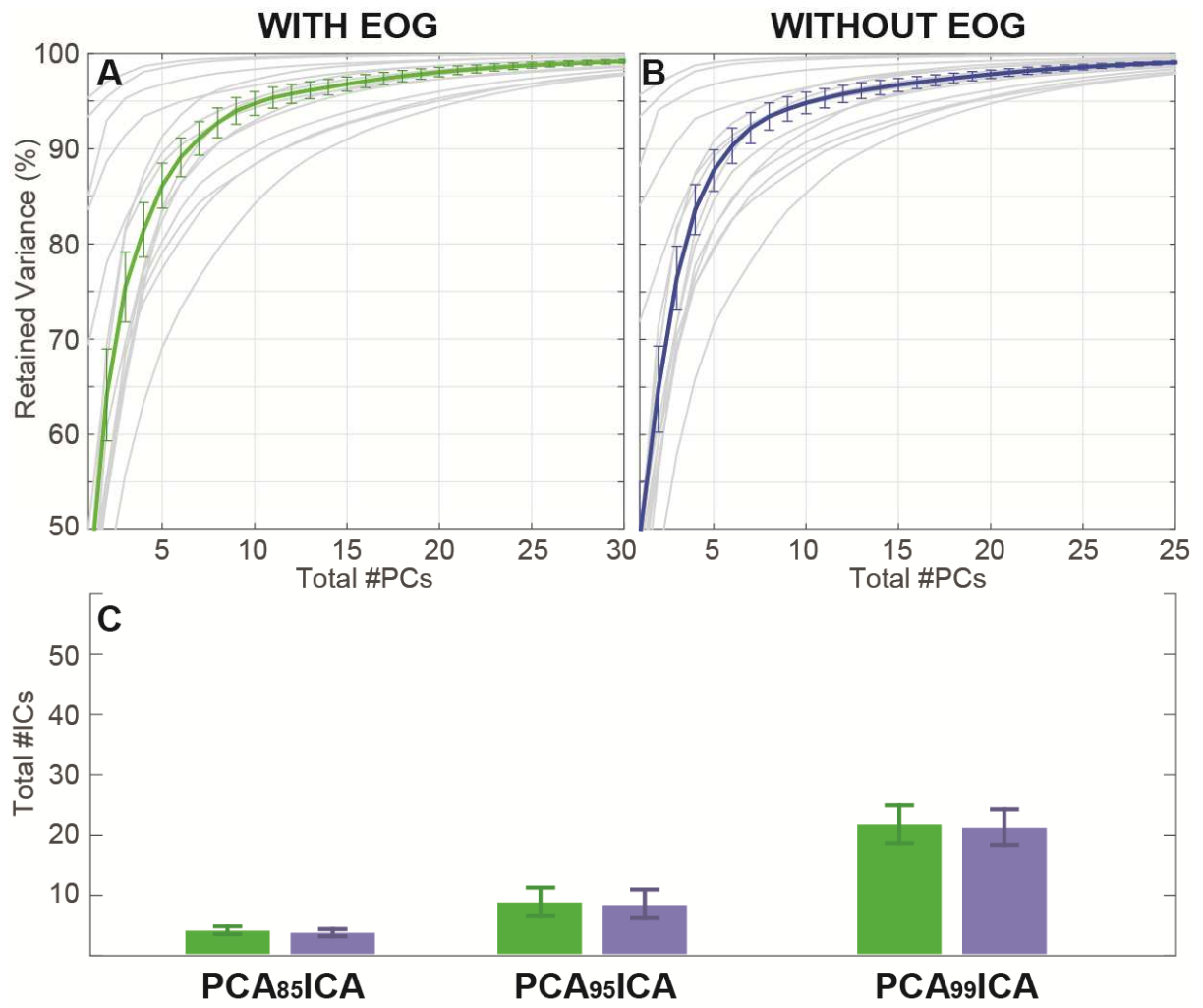
- 1 Hyvärinen, A., Oja, E., 2000. Independent component analysis: algorithms and applications. *Neural networks* 13,  
2 411-430.
- 3 Ivanenko, Y.P., Poppele, R.E., Lacquaniti, F., 2004. Five basic muscle activation patterns account for muscle  
4 activity during human locomotion. *The Journal of physiology* 556, 267-282.
- 5 Iversen, J.R., Makeig, S., 2014. MEG/EEG data analysis using EEGLAB. *Magnetoencephalography*. Springer,  
6 pp. 199-212.
- 7 Jung, T.-P., Humphries, C., Lee, T.-W., Makeig, S., McKeown, M.J., Iragui, V., Sejnowski, T.J., 1998.  
8 Removing electroencephalographic artifacts: comparison between ICA and PCA. *Neural Networks for Signal*  
9 *Processing VIII*, 1998. Proceedings of the 1998 IEEE Signal Processing Society Workshop. IEEE, pp. 63-72.
- 10 Jung, T.-P., Makeig, S., Humphries, C., Lee, T.-W., Mckeown, M.J., Iragui, V., Sejnowski, T.J., 2000.  
11 Removing electroencephalographic artifacts by blind source separation. *Psychophysiology* 37, 163-178.
- 12 Kambhatla, N., Leen, T.K., 1997. Dimension reduction by local principal component analysis. *Neural*  
13 *computation* 9, 1493-1516.
- 14 Kayser, J., Tenke, C.E., 2006. Consensus on PCA for ERP data, and sensibility of unrestricted solutions. *Clinical*  
15 *neurophysiology* 117, 703-707.
- 16 Kobayashi, T., Kuriki, S., 1999. Principal component elimination method for the improvement of S/N in evoked  
17 neuromagnetic field measurements. *IEEE Transactions on Biomedical Engineering* 46, 951-958.
- 18 Kothe, C.A., Makeig, S., 2013. BCILAB: a platform for brain-computer interface development. *Journal of*  
19 *neural engineering* 10, 056014.
- 20 Lagerlund, T.D., Sharbrough, F.W., Busacker, N.E., 1997. Spatial filtering of multichannel  
21 electroencephalographic recordings through principal component analysis by singular value decomposition.  
22 *Journal of clinical neurophysiology* 14, 73-82.
- 23 Makeig, S., Bell, A.J., Jung, T.-P., Sejnowski, T.J., 1996. Independent component analysis of  
24 electroencephalographic data. *Advances in neural information processing systems*, pp. 145-151.
- 25 Makeig, S., Debener, S., Onton, J., Delorme, A., 2004. Mining event-related brain dynamics. *Trends in cognitive*  
26 *sciences* 8, 204-210.
- 27 Makeig, S., Westerfield, M., Jung, T.-P., Enghoff, S., Townsend, J., Courchesne, E., Sejnowski, T.J., 2002.  
28 Dynamic brain sources of visual evoked responses. *Science* 295, 690-694.
- 29 McKeown, M.J., Makeig, S., Brown, G.G., Jung, T.-P., Kindermann, S.S., Bell, A.J., Sejnowski, T.J., 1997.  
30 Analysis of fMRI data by blind separation into independent spatial components. Naval Health Research Center,  
31 San Diego, CA.
- 32 Möcks, J., Verleger, R., 1986. Principal component analysis of event-related potentials: a note on misallocation  
33 of variance. *Electroencephalography and Clinical Neurophysiology/Evoked Potentials Section* 65, 393-398.
- 34 Muniz, A., Nadal, J., 2009. Application of principal component analysis in vertical ground reaction force to  
35 discriminate normal and abnormal gait. *Gait & posture* 29, 31-35.

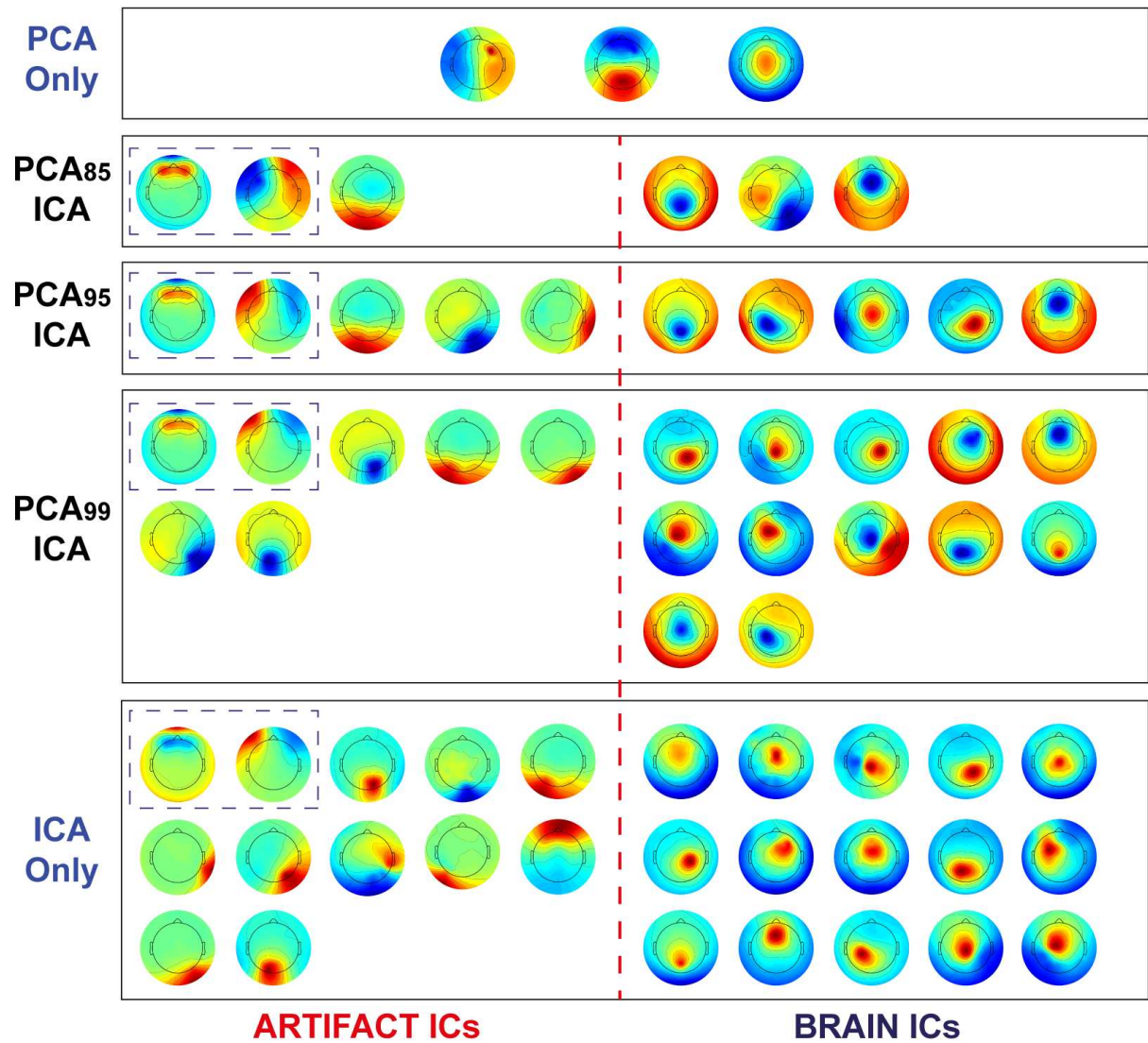
- 1 Nunez, P.L., 1981. A study of origins of the time dependencies of scalp EEG: I-theoretical basis. *IEEE*  
2 *Transactions on Biomedical Engineering*, 271-280.
- 3 Onton, J., Delorme, A., Makeig, S., 2005. Frontal midline EEG dynamics during working memory. *Neuroimage*  
4 27, 341-356.
- 5 Onton, J., Makeig, S., 2009. High-frequency broadband modulations of electroencephalographic spectra.  
6 *Frontiers in human neuroscience* 3.
- 7 Onton, J., Westerfield, M., Townsend, J., Makeig, S., 2006. Imaging human EEG dynamics using independent  
8 component analysis. *Neuroscience & Biobehavioral Reviews* 30, 808-822.
- 9 Oostenveld, R., Fries, P., Maris, E., Schoffelen, J.-M., 2011. FieldTrip: open source software for advanced  
10 analysis of MEG, EEG, and invasive electrophysiological data. *Computational intelligence and neuroscience*  
11 2011, 1.
- 12 Oostenveld, R., Oostendorp, T.F., 2002. Validating the boundary element method for forward and inverse EEG  
13 computations in the presence of a hole in the skull. *Human brain mapping* 17, 179-192.
- 14 Reid, S.M., Graham, R.B., Costigan, P.A., 2010. Differentiation of young and older adult stair climbing gait  
15 using principal component analysis. *Gait & posture* 31, 197-203.
- 16 Scherg, M., Von Cramon, D., 1986. Evoked dipole source potentials of the human auditory cortex.  
17 *Electroencephalography and Clinical Neurophysiology/Evoked Potentials Section* 65, 344-360.
- 18 Shiavi, R., Griffin, P., 1981. Representing and clustering electromyographic gait patterns with multivariate  
19 techniques. *Medical and Biological Engineering and Computing* 19, 605-611.
- 20 Silverman, B.W., 1986. Density estimation for statistics and data analysis. CRC press.
- 21 Sinharay, S., Stern, H.S., Russell, D., 2001. The use of multiple imputation for the analysis of missing data.  
22 *Psychological methods* 6, 317.
- 23 Staudenmann, D., Kingma, I., Daffertshofer, A., Stegeman, D.F., van Dieën, J.H., 2006. Improving EMG-based  
24 muscle force estimation by using a high-density EMG grid and principal component analysis. *IEEE Transactions*  
25 *on Biomedical Engineering* 53, 712-719.
- 26 Tadel, F., Baillet, S., Mosher, J.C., Pantazis, D., Leahy, R.M., 2011. Brainstorm: a user-friendly application for  
27 MEG/EEG analysis. *Computational intelligence and neuroscience* 2011, 8.
- 28 Vigário, R., Särelä, J., Oja, E., 1998. Independent component analysis in wave decomposition of auditory  
29 evoked fields. *ICANN 98*. Springer, pp. 287-292.
- 30 Whitmer, D., Worrell, G., Stead, M., Lee, I.K., Makeig, S., 2010. Utility of independent component analysis for  
31 interpretation of intracranial EEG. *Frontiers in human neuroscience* 4.
- 32 Winkler, I., Debener, S., Müller, K.-R., Tangermann, M., 2015. On the influence of high-pass filtering on ICA-  
33 based artifact reduction in EEG-ERP. *Engineering in Medicine and Biology Society (EMBC), 2015 37th Annual*  
34 *International Conference of the IEEE*. IEEE, pp. 4101-4105.

- 1 Winkler, I., Haufe, S., Tangermann, M., 2011. Automatic classification of artifactual ICA-components for  
2 artifact removal in EEG signals. Behavioral and Brain Functions 7, 30.  
3

ACCEPTED MANUSCRIPT

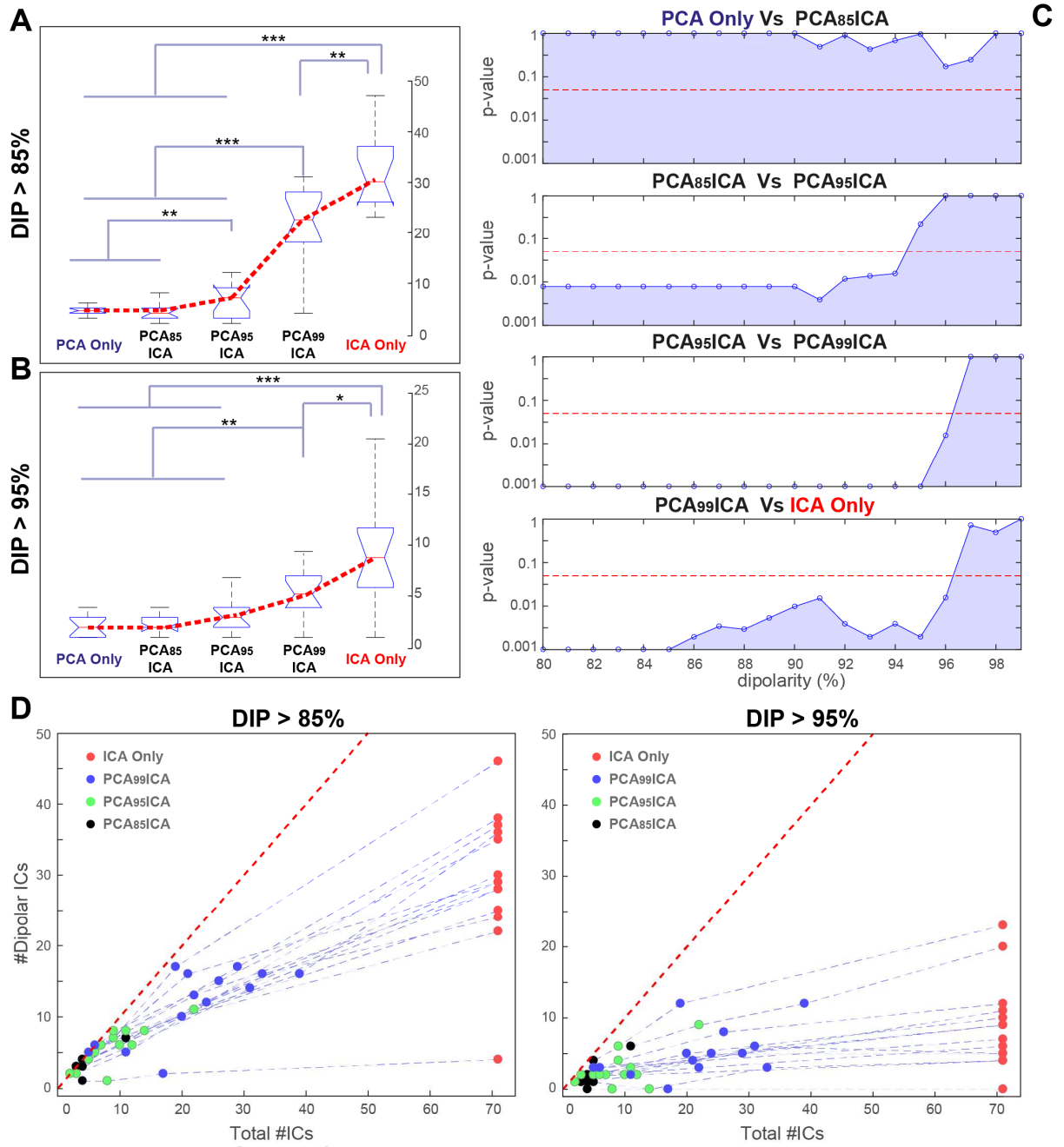


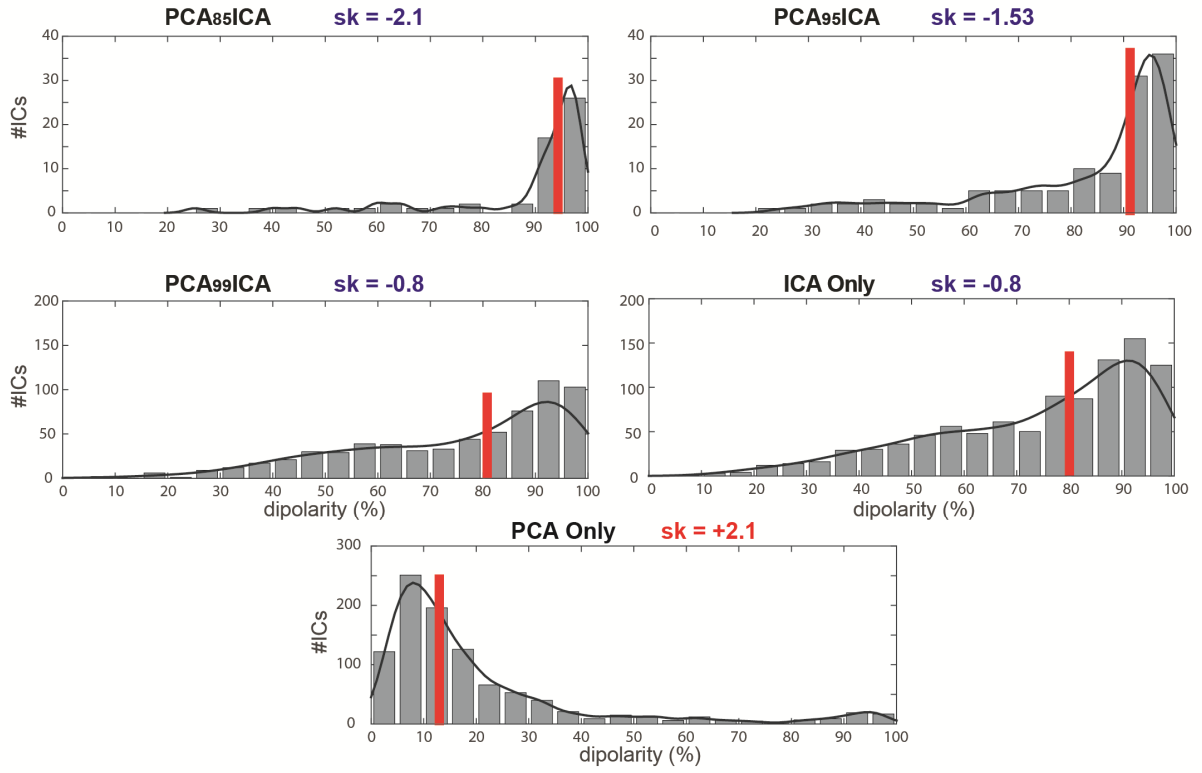


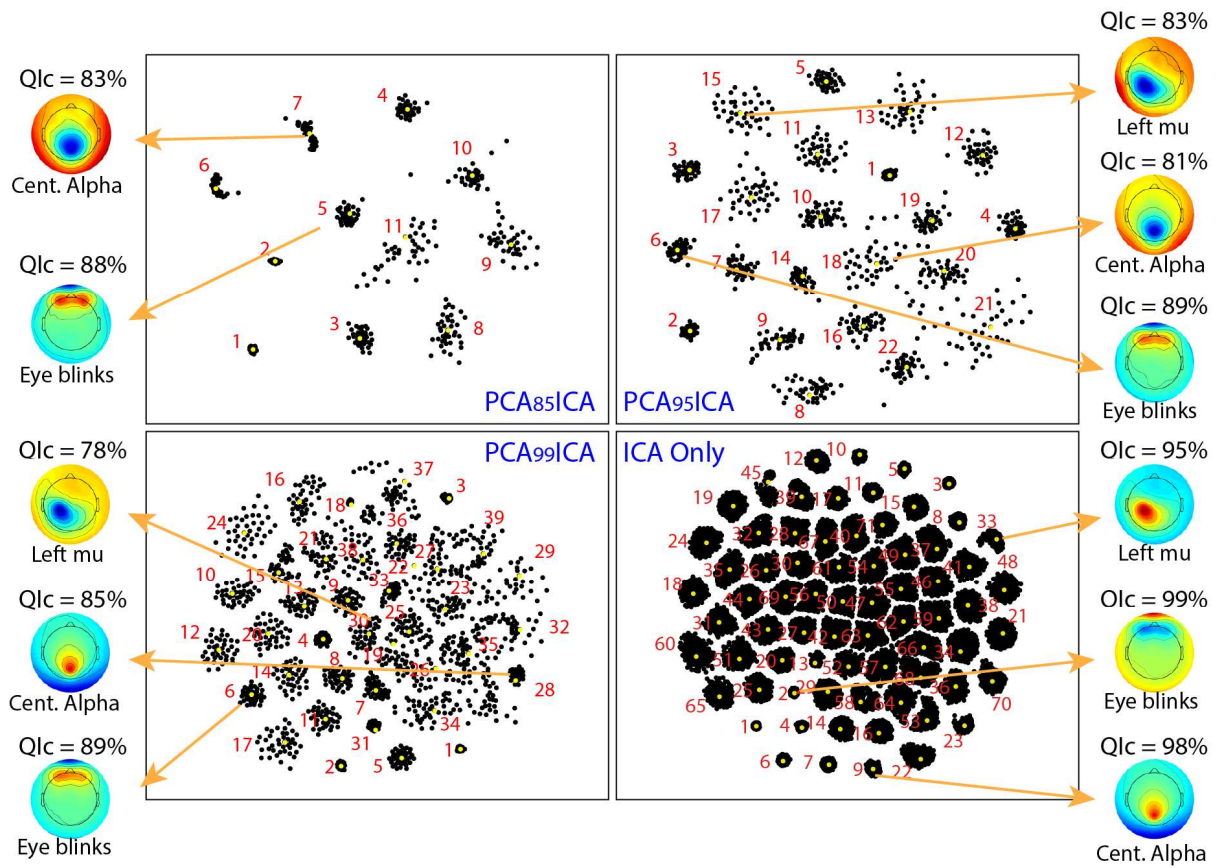


ARTIFACT ICs

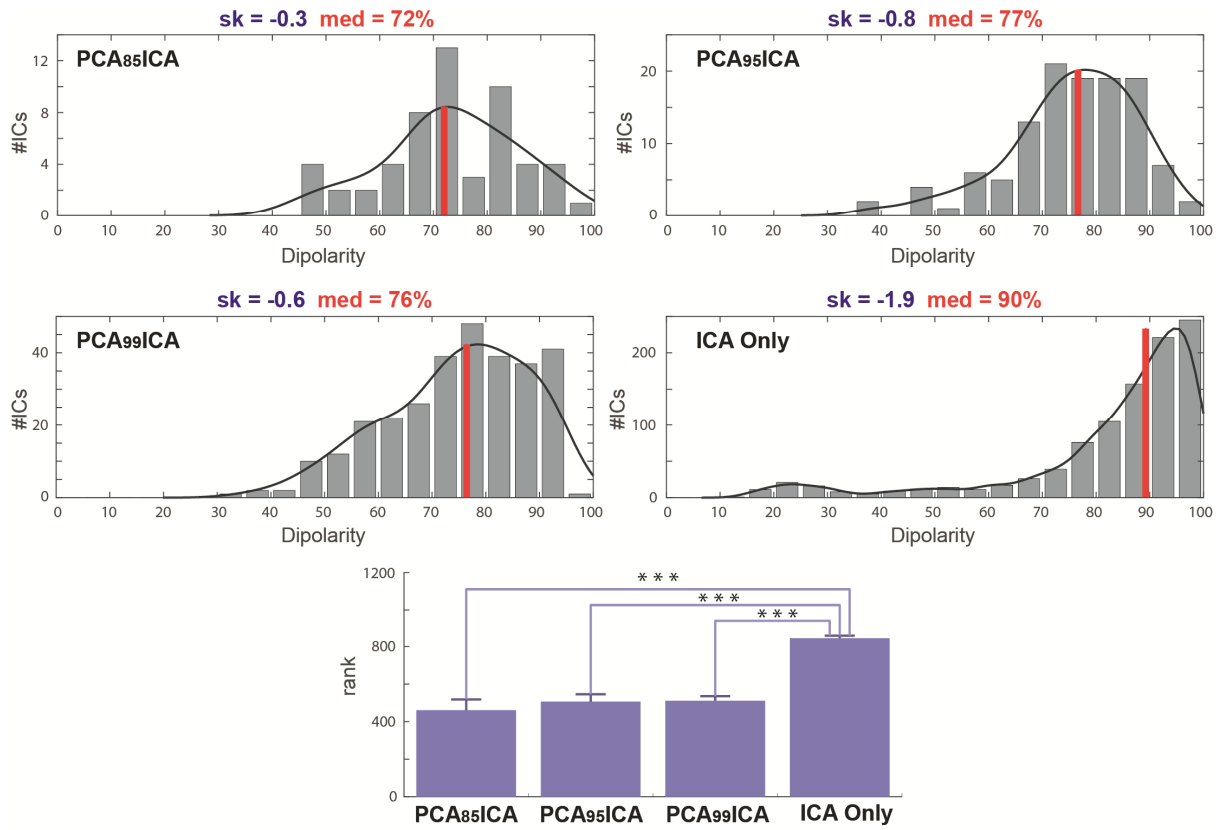
BRAIN ICs

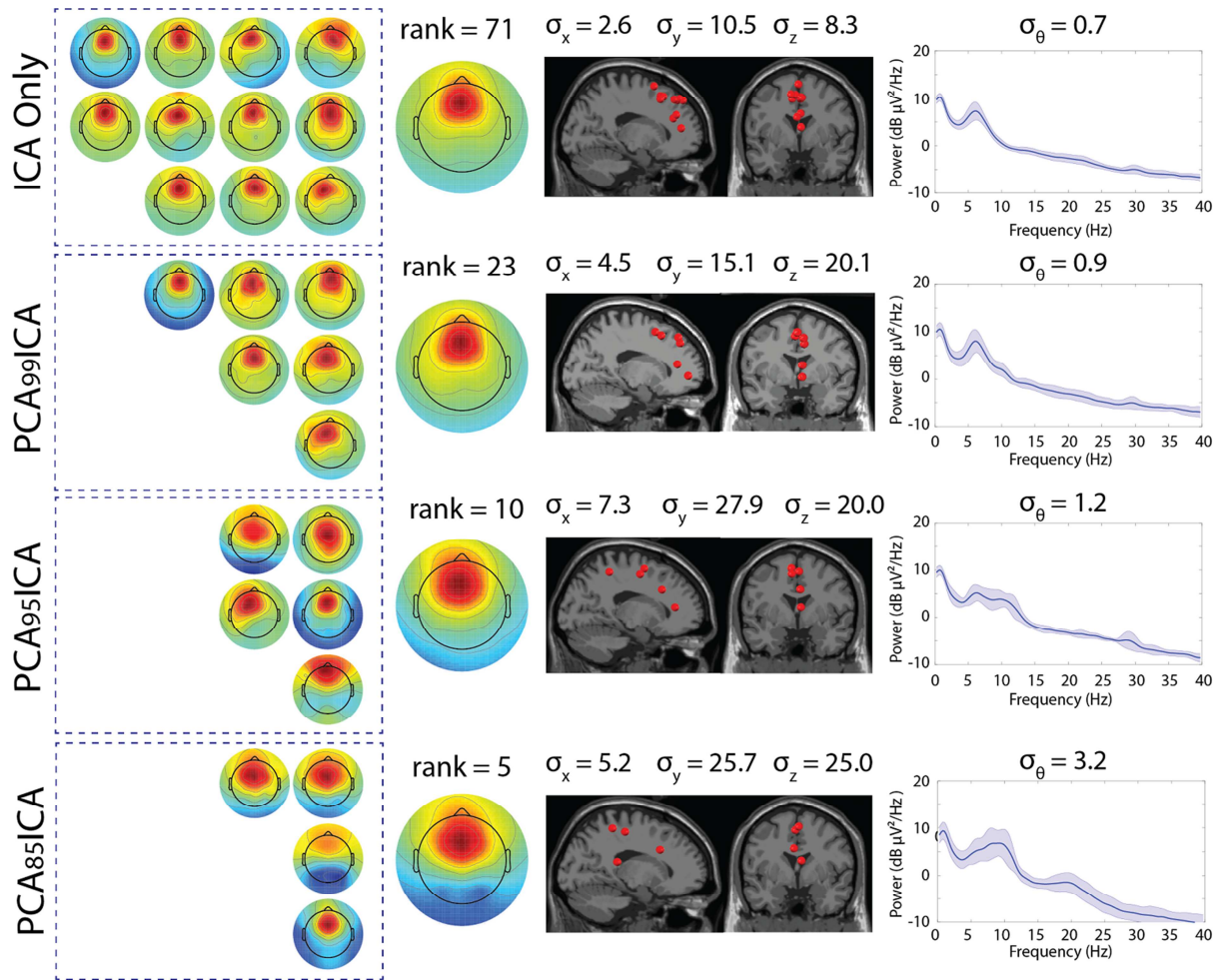






ACCEPTED M





ACCEPTED



